Information capacity and pattern formation in a tent map network featuring statistical periodicity

C. Hauptmann*

Centre for Nonlinear Dynamics in Physiology and Medicine, Department of Physiology, McGill University, 3655 Drummond Street, Montreal, Quebec, Canada H3G 1Y6

H. Touchette

Department of Physics and School of Computer Science, McGill University, Montreal, Quebec, Canada H3A 2A7

M. C. Mackey

Departments of Physiology, Physics, and Mathematics and Centre for Nonlinear Dynamics in Physiology and Medicine, McGill University, 3655 Drummond Street, Montreal, Quebec, Canada H3G 1Y6

We provide quantitative support to the observation that lattices of coupled maps are "efficient" information coding devices. It has been suggested recently that lattices of coupled maps may provide a model of information coding in the nervous system because of their ability to create structured and stimulus-dependent activity patterns which have the potential to be used for storing information. In this paper, we give an upper bound to the effective number of patterns that can be used to store information in the lattice by evaluating numerically its information capacity or information rate as a function of the coupling strength between the maps. We also estimate the time taken by the lattice to establish a limiting activity pattern.

Coupled map lattices (CMLs) have been recently elevated to the status of paradigm models for studying spatially extended systems composed of interacting units or agents such as populations of biological species [1,2] and plasma physics [3] (for a review see Ref. [4]). From the point of view of neural computation, CMLs also provide an interesting alternative to standard neural networks since they are capable of reproducing three important dynamical features of experimentally observed populations of neurons: (i) a rapid response to stimuli, (ii) a highly irregular or "chaotic" behavior of single neurons or small ensembles of locally coupled neurons, and (iii) a temporal cycling of the statistical activity of the entire population of neurons (statistical periodicity).

In a recent paper [2], Milton and Mackey have argued that these three properties of CMLs may provide a basis for hypothesizing neural information encoded in the spatiotemporal states of ensembles of neurons or in the overall distribution of activity of these neurons (ensemble coding), rather than in the temporal dynamics of individual neurons (temporal coding). Many aspects of biological neurons remain to be studied in order to prove or disprove this conjecture. However, CMLs provide on their own a tractable model with which many ideas and observations about neural information processing can be considered. In addition, it is suggestive to think that the chaotic behavior of individual neurons, modeled in CMLs at the level of the individual chaotic maps, is responsible for the high variability of activity patterns observed experimentally in ensembles of neurons, and for the high information capacity of these neuronal systems. Intuitively, however, there seems to be a trade-off involved, namely, (a) the ability of an ensemble of chaotic maps to converge rapidly to a steady state is proportional to the strength of the interaction which couples the different maps of a CML together, but (b) increasing the coupling strength too much is likely to reduce the overall activity and variability of the CML, and thereby reduce its information capacity.

Understanding how the coupling between the maps of a CML influences both of the above competing phenomena (rapid convergence and high capacity) is an important step toward establishing whether or not CMLs constitute a plausible model of neural information coding and storage.

In this paper, we study this technical issue by comparing two quantities which respectively measure the importance of each of the two competing phenomena. The first quantity is the information capacity (or information rate) which is defined, in the case of a CML, as the entropy of the joint probability density describing the steady-state activity of the CML divided by the number of maps composing the lattice. The information capacity, as we will see, is a direct correlate of the number of steady-state patterns which can be reached by any initial states of the CML. The other quantity of interest is the locking time of the network of maps, which is simply the time taken by the CML to reach a limiting activity pattern averaged over many initial configurations of the CML.

In the following, we evaluate both quantities numerically for a specific CML consisting of $n \times n$ tent maps arranged on a square lattice. The temporal evolution of each map in time is given by the equation

$$x_{t+1}^{i,j} = (1-\epsilon)S(x_t^{i,j}) + \frac{\epsilon}{4}[S(x_t^{i-1,j}) + S(x_t^{i,j-1}) + S(x_t^{i+1,j}) + S(x_t^{i,j+1})], \quad (1)$$

where

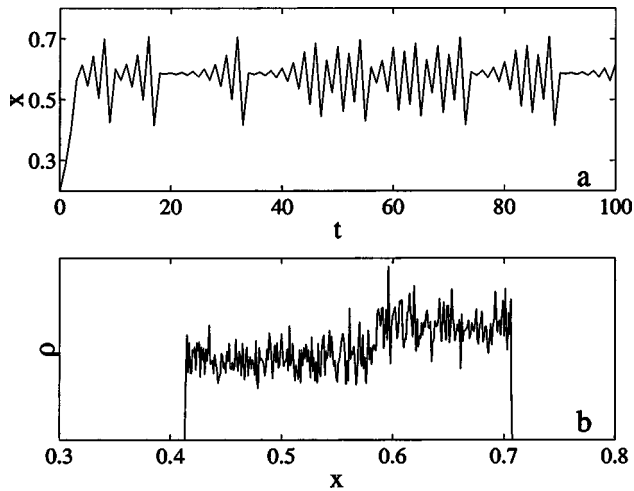*Corresponding author. Email address: chauptma@cnd.mcgill.ca

FIG. 1. Dynamics generated by an isolated tent map for a parameter $a = \sqrt{2}$. (a) Time series and (b) corresponding histogram representation obtained from a simulation with 40 000 steps.

$$S(x) = \begin{cases} ax, & 0 \le x < \dfrac{1}{2} \\[2mm] a(1-x), & \dfrac{1}{2} \le x \le 1. \end{cases} \qquad (2)$$

The indices i, j above denote the position of a specific map or *pixel* in the lattice $(1 \le i, j \le n)$, while t denotes the time. The coupling parameter $\epsilon \in [0,1]$ sets the interaction between the different pixels which, we assume, interact only with nearest neighbors (periodic boundary conditions are imposed). Finally, $a \in [0,2]$ is a parameter that controls the properties of the tent map.

To properly understand the significance of the two quantities that we intend to calculate (information capacity and locking time), and understand how these two quantities can compete with each other, it is instructive to review the properties of the isolated tent map $S(x)$, and, by a simple generalization, of the CML with $\epsilon = 0$ (more information can be found in Ref. [5–7]). More specifically, we have that the dynamics of the tent map alone is characterized by a Lyapunov exponent equal to $\ln a$. Thus, for $0 < a < 1$, all orbits of the map converge to the unique fixed point $x^* = 0$ independent of the value of the initial conditions, while for $a = 1$, all initial points of the map are fixed points. When $1 < a \le 2$, the dynamics of the tent map switches abruptly to a chaotic regime (see Fig. 1) characterized by a banded bifurcation diagram (Fig. 2) and a unique unstable fixed point located at $x^*(a) = a/(a+1)$. It is useful to note that the invariant density of the tent map, i.e., the density function of the invariant measure, is supported on subsets of the interval $[a(1-a/2), a/2]$ for $a < \sqrt{2}$, and has nonvanishing support on $[a(1-a/2), a/2]$ for $a \ge \sqrt{2}$ [8].

Behind the chaotic behavior of the temporal trajectory, the underlying regularity of the dynamics apparent in the banded structure of the bifurcation diagram is the signature of a property called statistical periodicity, which can be observed in the density distribution of an ensemble of tent maps
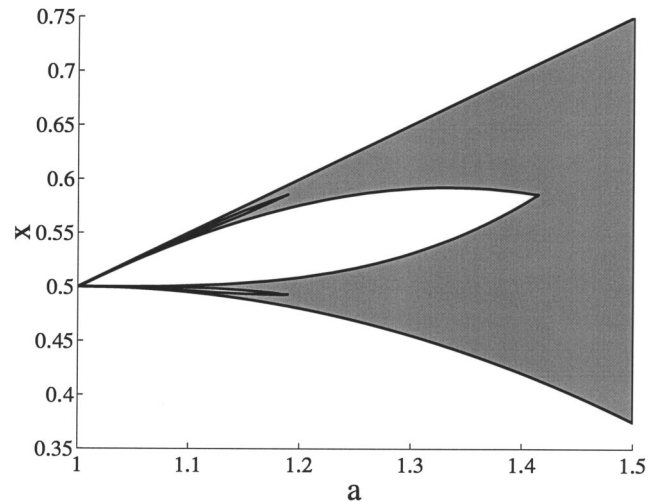

FIG. 2. Bifurcation diagram of the tent map showing the banded structure changing with varying parameter a. For $a = \sqrt{2}$, two bands merge to a continuum with an underlying structure not visible in this plot.

[2,6,7,9]. Specifically, for $2^{1/2^{1/(n+1)}} < a \le 2^{1/2^{1/n}}$, the densities of the tent map have periodicity with period $T = (n+1)$ for $n = 1, 2, \ldots$. Here, we always take $a = \sqrt{2}$ for our numerical simulations and computations.

The advantage of examining the density evolution of an ensemble instead of the temporal behavior of a single trajectory of an element originates in the different convergence times of these two processes. Typically the rate of convergence of densities is many orders of magnitude larger than for a single trajectory [2].

If an ensemble of noninteracting elements is considered, a histogram can be used to display the time evolution of the network activity. We do this by taking a large number of tent maps with different initial conditions. For each time step, we use the large number of state values to plot the normalized histogram and follow this (collapsed) density as a function of time (Fig. 3). The resulting density shows a cycle with period 2. In spite of the chaotic behavior within the bands, the banded structure shows a support of the system densities as they jump from one band to the other from one time step to the next.

In response to a given initial condition, the network [Eq. (1)] relaxes into a structurally ordered stable activity pattern (Fig. 4). Depending on the coupling strength, a stable activ-
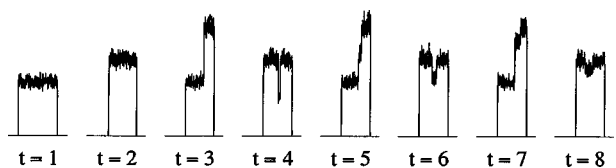

FIG. 3. The collapsed density prepared by iterating $N = 100\,000$ maps and calculating the density of states at each time step. The interval [0.2,0.8] is indicated by the horizontal line. The initial values were uniformly distributed on the interval [0.3,0.7] and the densities are normalized. Parameter: $a = \sqrt{2}$.
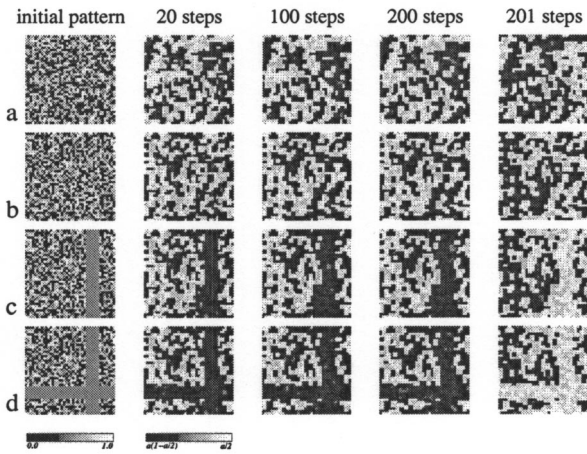
FIG. 4. Dynamic behavior of the tent map network in response to different inputs, Eq. (1). After a small number of steps, the network locks into a stable activity pattern. (a) initial pattern randomly chosen from the interval $[0,1]$, (b) another random initial pattern, (c) same as in (b) but with an additional stripe of initial value 0.5, (d) same as in (b) but with an additional cross of value 0.5. The plot represents system states $x \in [0,1]$ for the initial patterns and $x \in [a(1-a/2), a/2]$ for the simulated network patterns as indicated by the bars below in the figures. Parameters: $\epsilon = 0.2$, $a = \sqrt{2}$.
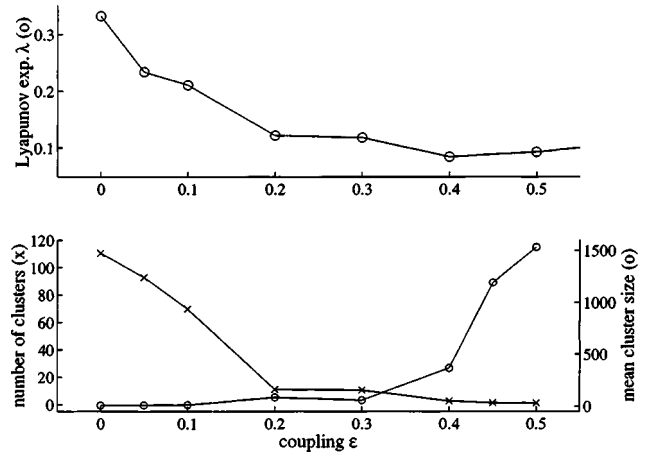

FIG. 5. The Lyapunov exponent (upper plot) and the number and size of the clusters (lower plot). The temporal spread of a tight density distribution of initial conditions for one network element is used to calculate the Lyapunov exponent [10]. The cluster size and number of clusters is calculated using a Hoshen-Kopelman algorithm [11]. Coarse grained network activity and 10 000 simulations with different seeds for the random number generator for each coupling strength are used. For the cluster detection algorithm, we take into account open boundary conditions.

ity structure is rapidly established and different initial patterns converge to different distinguishable limiting activity patterns. The period-2 oscillation observed for $a = \sqrt{2}$ in the collapsed density of the ensemble of uncoupled tent maps causes, in the coupled case, a switching from the activity pattern to its inverse pattern within one step (Fig. 4).

A numerical calculation of the Lyapunov coefficient of the single network element dynamics shows that even when the network is locked to a periodic activity pattern, the single element dynamics are still chaotic (Fig. 5). For the calculation of the Lyapunov exponent, the evolution of the trajectory of one network element as a function of time is investigated. The evolution is displayed using a histogram on the interval $[0,1]$ which is divided into 1000 bins. Starting with a tight density distribution of initial conditions (within one bin) for one element of the network, the temporal spread of this density distribution is quantified by the Lyapunov exponent. A total of 20 000 simulations are used to obtain the histogram of state evolution for one network element as a function of time [10]. Note that the theoretical value of the Lyapunov exponent in the uncoupled case is $\ln a = 0.347$.

A coarse graining approach allows us to separate the structure of the network activity, the fingerprint of statistical periodicity, from the chaotic activity of the network elements and represent it in a binary activity pattern. To do so, we must choose an appropriate threshold for the coarse graining. The unstable fixed point $x^\star = a/(a+1)$, for $a = \sqrt{2}$ where the two bands merge, seems to be a promising choice as a threshold for the coarse graining. Figure 6 shows the resulting binary pattern that is used to calculate the cluster size of the network. The mean size of the clusters, which is the mean number of connected network elements with the same

coarse grained state, increases with increasing coupling strength ϵ (Fig. 5 lower plot). In the case of coupling $\epsilon > 0.4$, the network tends to form one large cluster, while for coupling $\epsilon \leq 0.1$ the activity pattern consists of up to 100 clusters with a mean cluster size of $8-11$ elements per cluster.

Using the binary activity pattern, we are also able to calculate the probability of finding one element of the network in an *up* or *down* state if the neighboring elements are in a certain state configuration. This is the conditional probability distribution $p(x|x_{nn})$, where x indicates the state of a certain element of the network $x^{i,j}$ and x_{nn} the states of the next neighbors $x^{i+1,j}, x^{i,j+1}, x^{i-1,j}, x^{i,j-1}$. The conditional probability distribution can be calculated by evaluating the five-point joint probability distribution $p(x, x_{nn})$ and the four-neighbors joint probability distribution $p(x_{nn}) = \Sigma_x p(x, x_{nn})$. Hence, we obtain [12]

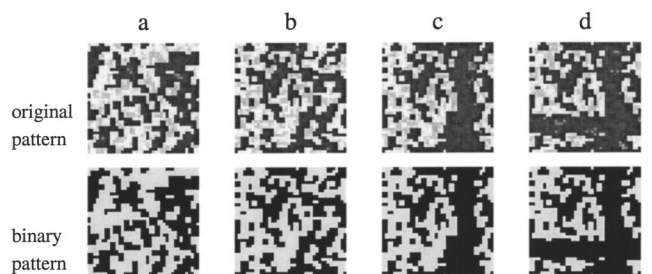$$p(x|x_{nn}) = \frac{p(x, x_{nn})}{p(x_{nn})}. \tag{3}$$

FIG. 6. Coarse grained network activity pattern. The threshold value used for the extraction of the binary pattern is the value of the unstable fixed point $x^\star$.
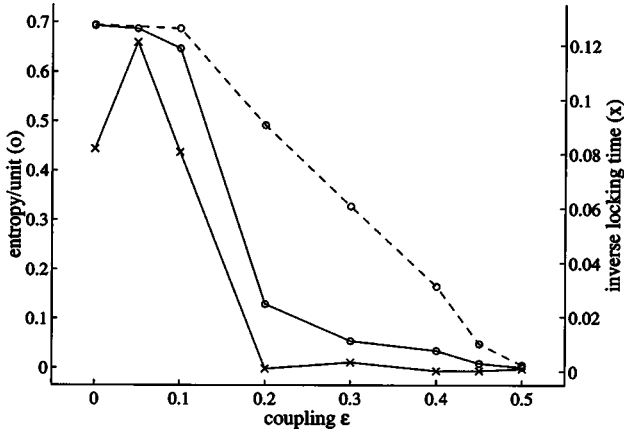
FIG. 7. Entropy per unit in natural units (open circle, full line) and the inverse of the locking time (cross, full line) as a function of the coupling strength ϵ. For the entropy calculation we evaluated the limiting pattern (after 20 000 simulation steps) of 20 000 simulations with different random initial conditions for each coupling strength. Ten remote elements of the network are used to calculate the conditional probability distribution. The dotted line indicates the entropy estimation obtained by using compression algorithms. For the locking time we evaluated the dynamics of 500 simulations with different initial conditions.

The nearest neighbor approximation is valid since only nearest neighbor coupling is considered. The conditional probability distribution allows us to calculate the entropy per network element,

$$H = -\sum_{x_{nn}} \sum_{x} p(x|x_{nn}) \ln p(x|x_{nn}). \qquad (4)$$

The entropy of a single network element calculated as described above gives a value for the uncertainty of the state of the element with respect to the states of the neighboring elements (Fig. 7). When we investigate binary states, we obtain a maximal uncertainty, or entropy, of $\ln 2$ if the probabilities of finding the network element in the two states are equal. The higher the value for the uncertainty the higher the information that can be obtained by knowing the state of the network element. Hence, the entropy per network element is proportional to the information capacity of the network.

As can be seen on Fig. 7, the entropy per network unit decreases here with increasing coupling strength ϵ starting with a maximal entropy of about $\ln 2$ in the uncoupled case. For weak coupling, the complexity of the local behavior is preserved, which results in a high entropy value, while for stronger network coupling, the binary states of the network units follow even more closely the corresponding states of the neighboring network elements.

In terms of information capacity, this means that for a certain coupling strength, say $\epsilon = 0.1$, we obtain an entropy per unit of $H = 0.6465$. Hence, the 40×40 network we have studied is able to realize $2^{1600H/\ln 2} \approx 2^{1500}$ different patterns in response to different initial patterns. We can also obtain an upper bound for the information that a pattern can store by applying the compression algorithm LZ77 [13,14] (used for

instance by gzip) to the files containing the binary activity patterns. This method of calculating the entropy is asymptotically equivalent to the statistical method of evaluating entropy when applied to infinitely long streams of data. The resulting compression ratio scaled in natural units validates our previous results (Fig. 7 dotted line). Furthermore, these results show that restricting the computation of probabilities to the next nearest neighbors is justified. These calculations are of use only if the structure of the network activity is stable and if the network activity rapidly relaxes onto the stimulus-dependent final state.

To investigate the time evolution of the activity pattern, we studied the correlation between the temporal coarse grained activity pattern and the limiting binary activity pattern (in our case after 20 000 simulation steps). We used the correlation function

$$r(t) = \frac{1}{N} \sum_{i,j} [x_{limiting}^{i,j} - x^{i,j}(t)]^2. \qquad (5)$$

Due to the statistical periodicity with period 2 when $a = \sqrt{2}$, the correlation oscillates with a period 2 and if the network locks to its limiting pattern, the correlation $r(t)$ oscillates between the two values 0 and 1. To define the locking time, we detected the first time step at which the correlation $r(t)$ was found to be smaller than a threshold value (0.01). This value can be interpreted as the reaction speed of the network in arbitrary units. In Fig. 7, it can be seen that the locking time increases with increasing coupling strength, and the formation of larger clusters in the strongly coupled regime takes several hundred simulation steps. The fastest network response is found in the weak coupling domain where the cluster size is small. Even in the uncoupled case, fast locking is observed which is induced by the effect of statistical periodicity.

In conclusion, we have shown that if the collapsed density displays statistical periodicity, then the information processing task is supported by two advantageous properties: the collapsed density converges rapidly towards a structurally ordered stable state and the information capacity of a network showing statistical periodicity is extremely high. The two quantities, information capacity and locking time, do indeed compete with each other, and there is an optimal value of the interaction parameter for which the lattice of coupled tent maps is capable of rapid convergence and simultaneously possesses a high information capacity.

Our investigations of a tent map network have also shown that despite the existence of chaotic temporal behavior in the single elements, the network shows several interesting behaviors. In response to an applied stimulus pattern the network relaxes onto an activity pattern, which shows a unique and stimulus-dependent limiting structure, while the dynamics of the single elements are still characterized by a positive Lyapunov exponent (Fig. 5). The analytic investigation of the dynamics of an isolated tent map [8] provides a way to coarse grain the activity pattern of the network into a binary pattern through the choice of a threshold value. The resulting binary pattern was studied in terms of its information capacity. The entropy of the single elements embedded in the net-

work decreases with increasing coupling ϵ (Fig. 7). The underlying reason for this behavior is a variation in the mean cluster size, which increases with increasing coupling strength until for $\epsilon=0.5$ only one large cluster is left. The evolution of the network activity is also characterized by the locking time, the number of steps required for the network to reach the limiting activity pattern (within a certain approximation). By comparing this locking time with the information capacity of the network, we have found that the best performance of the network was in the weak coupling domain $\epsilon=0.05$. Indeed, in this domain the network has a high information capacity due to the high single element entropy, the cluster size is small and a high number of clusters guarantees a large number of possible limiting activity patterns. Moreover, within 5–10 steps, the network obtains the limiting unique activity pattern and oscillates between the pattern and its inverse.

These network characteristics, though advantageous for a coding mechanism, leave many questions unanswered about the possibility that statistical periodicity be a viable mechanism for information storage in the nervous system. For instance, which part of the nervous system could detect such an activity pattern? What reads the code? Delayed systems have a special ability to detect periodicity. Due to this, we speculate that neuronal networks involving time delays are a promising candidate for a decoding device. How can experiments be designed to answer these questions and to investigate the relevance of the tent map network results in a more realistic neural network model? Experimental techniques with high spatiotemporal resolution are necessary to investigate these questions.

Despite many open questions, networks utilizing density coding and featuring statistical periodicity seem to be a promising candidate for answering questions about information coding and storage in the nervous system since systems with the properties we have examined have high information capacity and rapid convergence to limiting activity patterns.

[1] E.R. Caianiello, J. Theor. Biol. **2**, 204 (1961).

[2] J.G. Milton and M.C. Mackey, J. Neurophysiol. **94**, 489 (2000).

[3] E.D. Denman, J. Math. Anal. Appl. **21**, 242 (1968).

[4] J. Losson and M. Mackey, in *Stochastic and Spatial Structures of Dynamical Systems*, edited by S. van Strien and S. V. Lunel (North-Holland, Amsterdam, 1996), pp. 41–69.

[5] A. Lasota and M.C. Mackey, *Chaos, Fractals and Noise: Stochastic Aspects of Dynamics* (Springer, New York, 1994).

[6] J. Losson and M.C. Mackey, Phys. Rev. E **50**, 843 (1994).

[7] J. Losson and M.C. Mackey, Phys. Rev. E **52**, 115 (1995).

[8] T. Yoshida, H. Mori, and H. Shigematsu, J. Stat. Phys. **31**, 279 (1983).

[9] N. Provatas and M.C. Mackey, Physica D **53**, 295 (1991).

[10] J.-P. Eckmann and D. Ruelle, Rev. Mod. Phys. **57**, 617 (1985).

[11] J. Hoshen and R. Kopelman, Phys. Rev. B **1**, 3438 (1976).

[12] T.M. Cover and J.A. Thomas, *Elements of Information Theory* (Wiley, New York, 1991).

[13] J. Ziv and A. Lempel, IEEE Trans. Inf. Theory **23**, 337 (1977).

[14] J. Ziv and A. Lempel, IEEE Trans. Inf. Theory **24**, 530 (1978).